Ultrasonic Detection of Cracks in Studs and Bolts Using Dynamic Predictive Deconvolution and Wave Shaping

*Dong-Man Suh, **Whan-Woo Kim, ***Dae-Yen Kim, and ***Jin-Gyun Chung

Abstract

Bolt degradation has become a major issue in the nuclear industry since the 1980's due to failure during operation. If small cracks in stud bolts are not detected early enough, they grow rapidly and cause catastrophic disasters. Their detection, despite its importance, is known to be a very difficult problem due to the complicated structures of the stud bolts. This paper presents a method of detecting and sizing a small crack in the root between two adjacent crests in threads. The key idea is from the fact that the Rayleigh wave propagates slowly along a crack from the tip to the opening and is reflected from the opening mouth. When there exists a crack, a small delayed pulse due to the Rayleigh wave is detected between large regularly spaced pulses from the thread. The delay time is the same as the propagation delay time of the slow Rayleigh wave and is proportional to the size of the crack.

To efficiently detect the slow Rayleigh wave, three methods based on digital signal processing are proposed: modified wave shaping, dynamic predictive deconvolution, and dynamic predictive deconvolution combined with wave shaping.

I. Introduction

In industrial facilities such as nuclear power plants, many kinds and sizes of bolts are used. But their degradation has become a major issue in the nuclear industry since the 1980's due to the failure during operation [1]-[4].

Generally, ultrasonic, magnetic particle and eddy current testing procedures are carried out for bolt inspections. Among these, ultrasonic inspection is the only one which is expected to detect cracks in the thread region, without removing the studs and bolts. However, by conventional ultrasonic testing methods, it is difficult to detect flaws such as stress-corrosion cracks or corrosion wastage in the threads. In many cases, a small flaw signal can hardly be distinguished from the complicated signals reflected from threads. When the flaw is quite small, the signal amplitude reflected from it is nearly equal in size to the typical noise signal.

In our new methods, the small, weak signals from Rayleigh waves propagating along the crack face to its opening in a bolt thread are useful for not only detecting the crack but also sizing it. This signal, appearing after one of the regularly spaced thread echos, can be used to resolve the location and the size of a small crack in the stud and bolt threads.

To determine the location and the size of a small crack in the stud and bolt threads using Rayleigh waves, it is important to enhance the sharpness of ultrasonic waveforms. To this end, a modified wave shaping method is proposed which is based on the method in [5]. Also, to remove the strong multiple reflections from the regular structure of bolt threads, a dynamic predictive deconvolution method is proposed. These two methods can be combined to clearly show the location and size of a crack.

II. Crack Sizing by Tip Wave and Rayleigh Wave

Among the two techniques in the conventional pulse-echo method, the shear-wave, angle-beam technique is suitable for the studs with center-drilled holes, while the longitudinal-wave, normal-beam, or longitudinal-wave angle-beam technique is suitable for the stud bolts and nuts without center-drilled holes.

When an ultrasonic beam travels into a thread region, there is almost identical interval (delay time) between echoes from any two successive threads, as is schematically shown in Fig. 1. If the incident beam is perpendicular to the flank of a thread, the pulse-echo signal will be dominated by a strong backscattered reflection from the flank, with the weaker diffracted waves from the thread root ar-

* Department of Electrical Engr., Kunjang College.
** Department of Electronics Engr., Chungnam National Univ.
*** Department of Inform. & Comm. Engr., Chonbuk National Univ.

Manuscript Received: January 26, 1998.

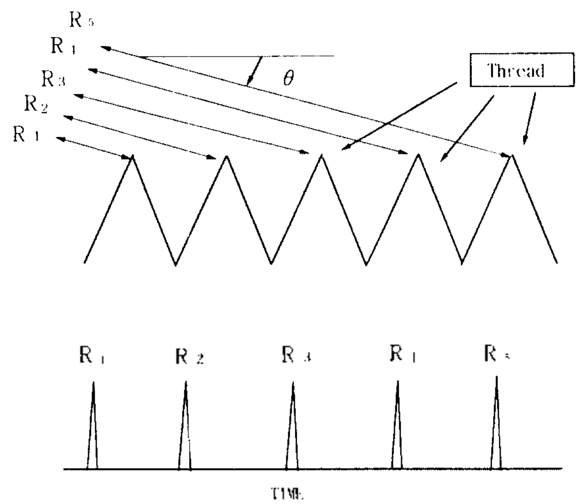

Figure 1. Schematic showing ray paths for reflections from roots of threads.

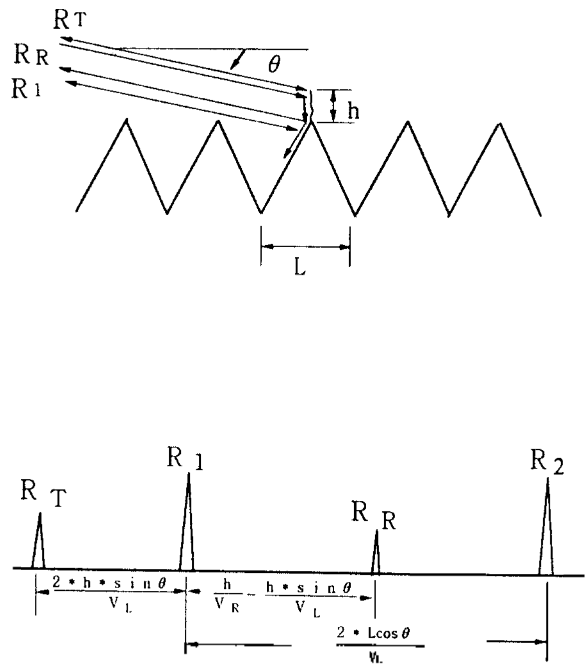

Figure 2. Schematic showing ray paths for reflections from a crack at the root of a thread.

riving at the same time. If the incident beam angle to the flank of a thread is other than 90 degrees, the reflected ultrasonic energy from the flank of the thread will not be strongly detected in a pulse-echo measurement. Thus the tip diffracted root signal will be the major response. Actually, the thread signals become smaller and less recognizable while propagating through the bolt due to ultrasonic attenuation and noise in the medium. But we can detect and size a small crack from the small signals between the thread signals as follows. If bolt threads are in good condition without any crack, the time intervals between the arrival times of the reflected signals from any two successive threads are identical. But if there is a small crack in the thread which starts at the base of the thread root and proceeds at right angles to the bolt axis, the delay times of signals from such a thread root are different from those of normal thread signals.

Fig. 2 provides further detail in this situation for the case of longitudinal-wave, angle-beam illumination. When an angled ultrasonic beam encounters a crack in the root of a thread, some of the energy is converted into various waves diffracted or reflected from the tip of the crack and from the intersection of the thread root and crack, as shown in Fig. 2. The relevant echoes are: R_T, which is diffracted by the crack tip, R_1, which diffracts from the intersection of the crack and the root of thread, and R_R, which travels as a Rayleigh wave along the crack face and radiates from the mouth where the crack opens at the root of the thread. The signal, R_1, from the thread is enhanced by the presence of the crack, but its path length, and hence the arrival time, is almost unchanged from the crack free case. The tip signal R_T precedes R_1 and the Rayleigh wave R_R occurs after the main echo R_1. Thus we can estimate the crack size from the delay time of either of these signals.

Consider the Rayleigh wave delay time Δt_R of the signal R_R. By simple reasoning, it can be seen that the delay time by which R_R follows R_1 is given by

$$\Delta t_R = h/V_R - h \sin \theta / V_L, \tag{1}$$

so that the crack height can be estimated by

$$h = \Delta t_R V_R V_L / (V_L - V_R \sin \theta), \tag{2}$$

where Δt_R = delay time between the thread root and the Rayleigh wave signal, V_R = Rayleigh wave velocity (2800 m/sec in steel), V_L = longitudinal wave velocity (5800 m/sec in steel), θ = angle between incident wave and bolt axis and h = crack size. Also, we can estimate the crack size by the delay time Δt_T between the tip diffracted signal R_T and the main signal R_1. It can be easily seen that the delay time between these echoes is given by

$$\Delta t_T = 2h \sin \theta / V_L, \tag{3}$$

so that the crack height can be estimated by

$$h = \Delta t_T V_L / (2 \sin \theta), \tag{4}$$

where Δt_T = delay time between the tip-diffracted signal and the thread root signal. On the other hand, when using the shear-wave, angle-beam technique to detect a small crack in the thread root, one should substitute the shear velocity V_T in place of the longitudinal wave velocity V_L in (1)-(4).

To verify the theory, a carbon steel test specimen was fabricated with threads, and notches were machined into the test specimen locations shown in Fig. 3. The pitch-to-pitch interval is 3 mm. The notches are produced by EDM techniques with 0.5, 1.0, 2.0, and 3.0 mm depth, 0.2 mm width, and 3.0 mm length. We have to select the center frequency of the transducer properly in order to discriminate successive thread echoes. The center frequency of the transducer must be greater than twice the pulse train frequency of the thread signals. When the pitch-to-pitch distance is 3 mm and the angle between the incident wave and the thread wall is nearly zero in the longitudinal-wave, straight-beam case, the pulse train frequency from threads is approximately 1 MHz in pulse-echo technique. In the 60 degree shear-wave, angle-beam technique, the pulse train frequency from threads is approximately 0.5 MHz. The center frequency of transducers used in the test, 10 MHz, thus satisfies the above criteria and also gives good resolution.

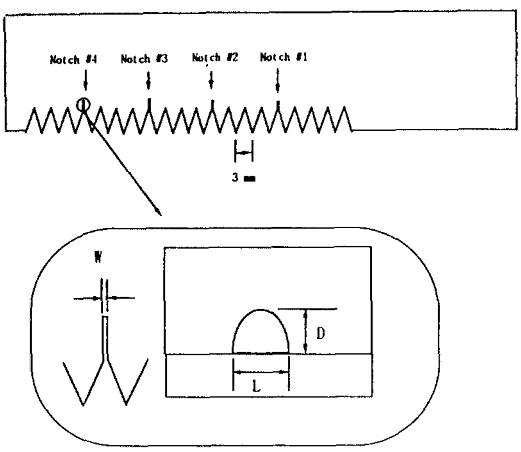

Notch #	L(mm)	D(mm)	W(mm)
1	3.0	0.5	0.2
2	3.0	1.0	0.2
3	3.0	2.0	0.2
4	3.0	3.0	0.2

Figure 3. Dimensions of the test specimen.

Fig. 4 shows the A-scan display of the signals from stud threads containing the notches as observed by the longitudinal-wave, straight-beam technique. Threads with notches 0.5 mm deep produced very low amplitude signals, while those with 1.0, 2.0, 3.0 mm notches produced higher amplitude signals than the notch free threads noise. An expanded A-scan display showing the 0.5 mm notch signal is in Fig. 4(a). The notch signal R_1 is reflected from the corner of the crack and thread root. As there is a small crack at the thread root, the signal R_R, which travels as a Rayleigh wave along the crack face and radiates from the crack mouth occurs after the thread signal R_1. But since the tip diffracted signal R_T almost overlaps the R_1 signal in time and is very weak in amplitude, it is not resolved.

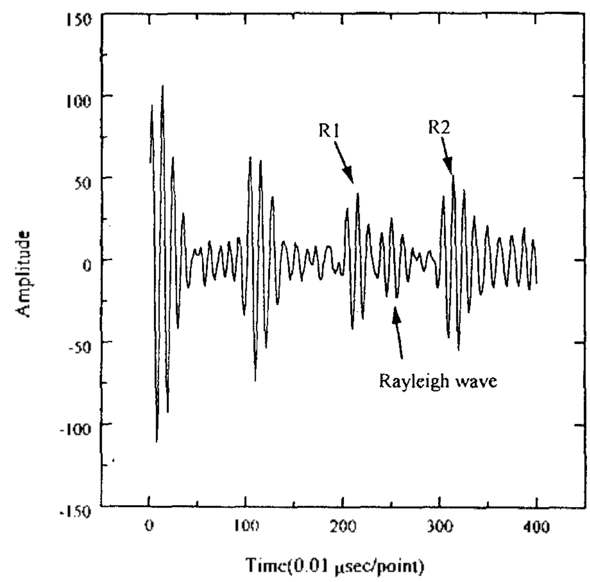

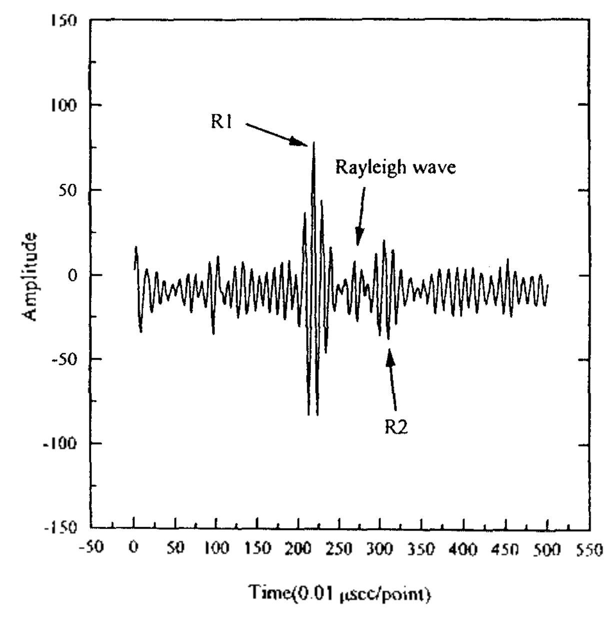

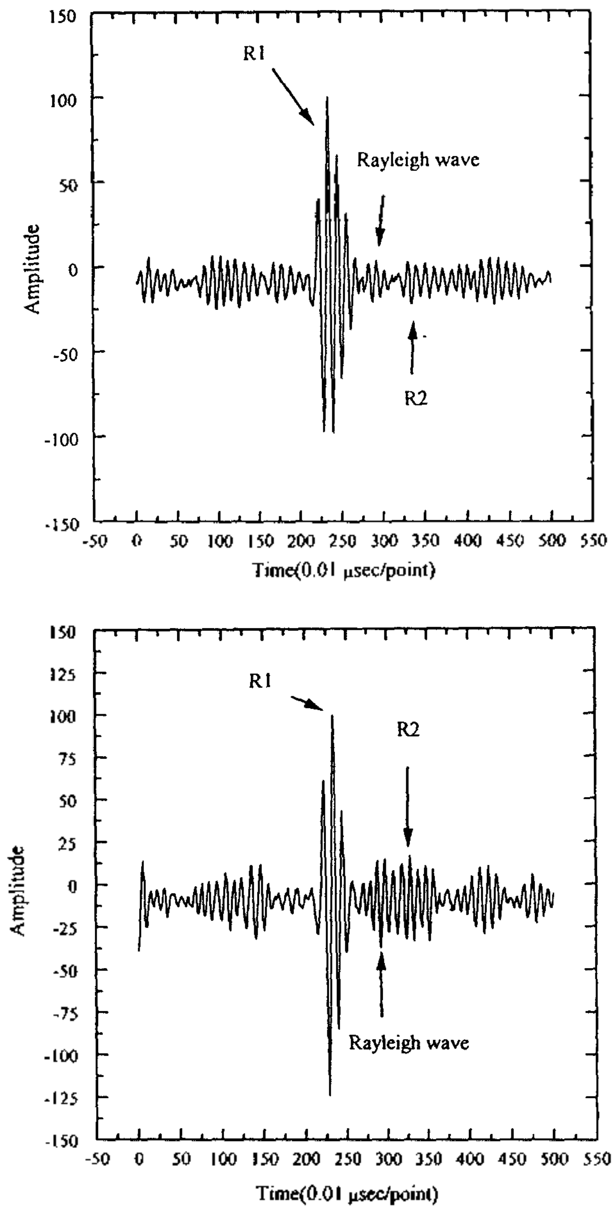

Figure 4. Ultrasonic signals from threads with notches using the longitudinal-wave, straight-beam technique; (a) 0.5 mm notch, (b) 1.0 mm notch, (c) 2.0 mm notch, (d) 3.0 mm notch.

For the 1-mm notch, as shown in Fig. 4(b), the signal R_R is again seen. In addition, the signal R_1 is much larger than R_2. These trends continue in Figs. 4(c) and (d). In particular, the amplitude of the trailing thread signal R_2 is decreased because the sound path is interrupted by the notch. As the crack size increases, the echo amplitude of the signal R_2 decreases and eventually disappears due to the acoustic shadowing. But the Rayleigh wave appears after the notch signal R_1 in Figs. 4(b), (c) and (d). From Fig. 4, the crack size can be determined by (2).

For the shear-wave, angle-beam examination, a 60-degree transducer was used. Figs. 5(a) and (b) show the thread signals with 2.0 and 3.0 mm deep notches. The notched thread signal R_1 is reflected at the corner of the notch and thread root. In Figs. 5(a) and (b), the Rayleigh wave R_R appears after the notch signal R_1. However, it was difficult to discriminate Rayleigh wave signals R_R after R_1 for 0.5 mm and 1.0 mm notches.

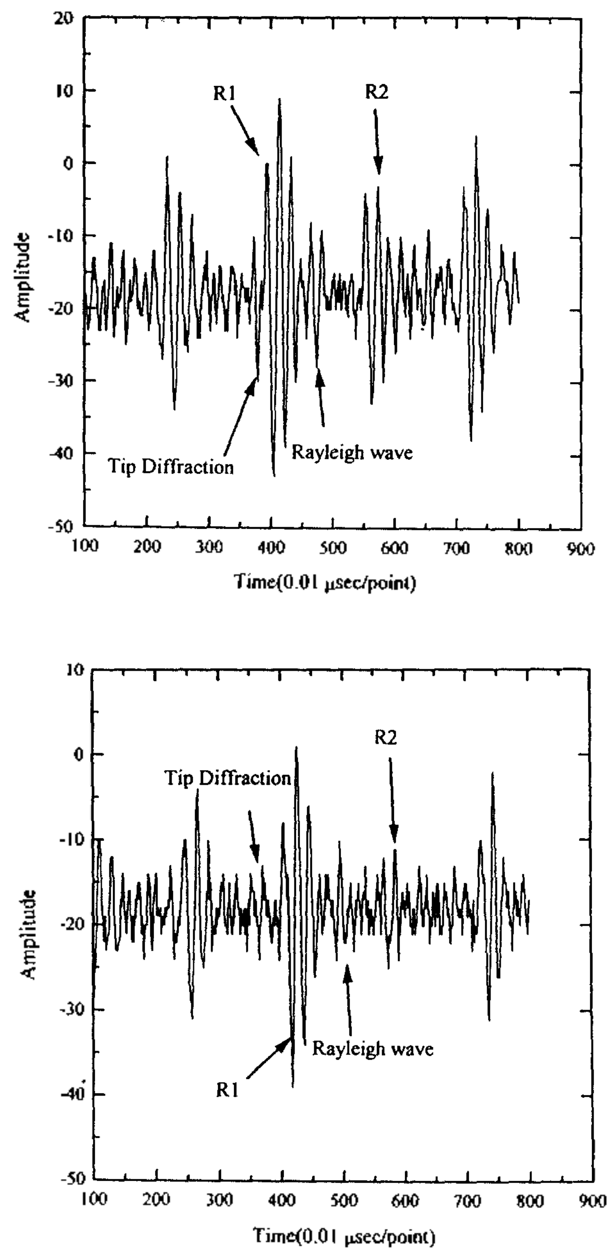

Figure 5. Ultrasonic signal from threads with notches using the shear-wave, angle-beam technique; (a) 2.0 mm notch, (b) 3.0 mm notch.

Ⅲ. Digital Wave Shaping by Modified Least Squares Method

To determine the location and the size of a small crack in the stud and bolt threads, it is important to enhance the sharpness of ultrasonic waveforms. In this section, a wave shaping method is presented to improve the resolution of the system based on the signal from a reference. A similar technique was used in [5] and our technique is a more generalized one [6].

A. Conventional Wave Shaping Technique

Given a reference signal $a(n)$, we want to find the mathematical operator $f(n)$ that will transfer $a(n)$ into a desired waveform $d(n)$ by the convolution of $a(n)$ with $f(n)$, i.e.,

$$d(n) = a(n) * f(n), \tag{5}$$

where (*) means the convolution operation. However, the finite length of $f(n)$ will introduce errors and consequently the waveform $q(n)$ computed by the convolution of $a(n)$ with the finite-length $f(n)$ is not equal to the desired waveform $d(n)$. When the length of $f(n)$ is $m+1$, $q(n)$ is computed as

$$q(n) = \begin{cases} \sum_{s=0}^{m} f(s)a(n-s), & n = 0, 1, \cdots, m+N, \\ 0, & n > m_N, \end{cases} \tag{6}$$

where $N+1$ is the length of the reference waveform. Thus it is necessary to obtain the optimized coefficients of the finite-length $f(n)$ that will result in as small an error as possible. In this paper, the error is defined in the least-squares sense as

$$E = \sum_{n=0}^{\infty} (d(n) - q(n))^2. \tag{7}$$

From (6) and (7), error E can be expressed as

$$E = \sum_{n=0}^{m+N} \left(d(n) - \sum_{s=0}^{m} f(s)a(n-s)\right)^2 + \sum_{n=m+N+1}^{\infty} d(n)^2. \tag{8}$$

The optimized coefficients of $f(n)$ can be found by minimizing the error E in (8). By

$$\frac{\partial E}{\partial f(n)} = 0, \quad n = 0, 1, \cdots, m, \tag{9}$$

we obtain

$$\sum_{s=0}^{m} f(s) \sum_{n=0}^{m+N} a(n-s)a(n-j) = \sum_{n=0}^{m+N} d(n)a(n-j),$$

$$j = 0, 1, \cdots, m. \tag{10}$$

By defining r_{j-s} and g_j as

$$\begin{aligned} r_{j-s} &= \sum_{n=0}^{m+N} a(n-s)a(n-j), \\ g_j &= \sum_{n=0}^{m+N} d(n)a(n-j), \end{aligned} \tag{11}$$

(10) can be expressed as

$$\sum_{s=0}^{m} f(s) r_{j-s} = g_j, \quad j = 0, 1, \cdots, m. \tag{12}$$

Notice that r_{j-s} is the autocorrelation of $a(n)$ and g_j is the correlation of $d(n)$ with $a(n)$. Thus the optimized coefficients of $f(n)$ can be obtained by solving the following matrix equation:

$$\begin{bmatrix} r_0 & r_1 & \cdots & r_m \\ r_1 & r_0 & \cdots & r_{m-1} \\ \vdots & \vdots & \ddots & \vdots \\ r_m & r_{m-1} & \cdots & r_0 \end{bmatrix} \begin{bmatrix} f(0) \\ f(1) \\ \vdots \\ f(m) \end{bmatrix} = \begin{bmatrix} g_0 \\ g_1 \\ \vdots \\ g_m \end{bmatrix}. \tag{13}$$

The minized error will then be

$$E_{\min} = \sum_{n=0}^{\infty} d(n)^2 - \sum_{n=0}^{m} f(n)g(n). \tag{14}$$

B. Wave Shaping by Modified Least Squares Method

Even if the operator is computed by (13) using a reference signal from a root of threads without any crack, the performance of the operator is not satisfactory in some cases due to the minute differences between the signals from threads. The performance can be improved significantly by the following modified least squares method.

If we use two reference signals $a_1(n)$ and $a_2(n)$ from threads without any cracks, the error E in (8) can be rewritten as

$$E = \sum_{n=0}^{m+N} \left(2d(n) - \sum_{s=0}^{m} f(s)a_1(n-s) - \sum_{s=0}^{m} f(s)a_2(n-s)\right)^2 + \sum_{n=m+N+1}^{\infty} d(n)^2. \tag{15}$$

To obtain optimized operator coefficients, (9) is applied to (15), which gives

$$2\left(\sum_{n=0}^{m+N} d(n)a_1(n-j) + \sum_{n=0}^{m+N} d(n)a_2(n-j)\right)$$
$$= \sum_{s=0}^{m} f(s)\left[\sum_{n=0}^{m+N} a_1(n-s)a_1(n-j) + \sum_{n=0}^{m+N} a_2(n-s)a_1(n-j)\right.$$

$$+\sum_{n=0}^{m+N} a_1(n-s)a_2(n-j)+\sum_{n=0}^{m+N} a_2(n-s)a_2(n-j)\Bigg],$$

$$j=0,\ 1,\ \cdots,\ m. \tag{16}$$

Using (11), (16) can be represented as

$$\sum_{s=0}^{m} f(s)[r_{11(j-s)}+r_{21(j-s)}+r_{12(j-s)}+r_{22(j-s)}]$$

$$=2[g_{1(j)}+g_{2(j)}],\ j=0,\ 1,\ \cdots,\ m, \tag{17}$$

where r_{kl} is the correlation of $a_k(n)$ with $a_l(n)$ and g_k is the correlation of $d(n)$ with $a_k(n)$. The optimized operator can be obtained from (17) and the minimized error will be

$$E_{\min}=4\sum_{n=0}^{\infty} d(n)^2-3\sum_{s=0}^{m} f(s)[g_{1(s)}+g_{2(s)}]$$

$$+\sum_{n=0}^{m+N}\Bigg[\sum_{s=0}^{m} f(s)a_1(n-s)\sum_{s=0}^{m} f(s)a_2(n-s)\Bigg]. \tag{18}$$

In general, when the number of reference waveforms is α, the optimized operator can be obtained from the following:

$$\sum_{s=0}^{m} f(s)\sum_{l=1}^{\alpha}\sum_{k=1}^{\alpha} r_{lk(j-s)}=\alpha\sum_{l=1}^{\alpha} g_{l(j)},\quad j=0,\ 1,\ \cdots,\ m. \tag{19}$$

C. Experimental Results

Fig. 6 shows an ultrasonic signal obtained from threads with a crack. The center frequency of the transducer is 10 MHz. In this case, as can be seen from the figure, it is difficult to detect a Rayleigh wave. To apply our wave shaping method to this case, the desired signal in Fig. 7 is used. The desired signal in Fig. 7 is a portion of the reflected signal from the first thread root in Fig. 6 with negative part truncated properly. Two reference signals were used to find the optimized operator coefficients. Thus the optimized operator coefficients are obtained from (19) with $\alpha=2$. By applying the operator to the signal in Fig. 6, the processed signal is obtained as shown in Fig. 8. From Fig. 8, the small crack can be easily detected.

As the ultrasonic waves continue to propagate through a material, the waves experience exponential-type attenuation. To compensate for this, we use the concept of window by which each wave is normalized to unity, as can be seen in Fig. 8.

Ⅳ. Dynamic Predictive Deconvolution

As can be seen from Fig. 1, ultrasonic signals from studs and bolts have strong reflections from roots of threads. To efficiently determine the location and the size of a small crack, these large regularly spaced pulses can be removed by predictive deconvolution technique [7]. Based on the fact that the large regularly spaced pulses are correlated with each other, the predictive deconvolution estimates the next signal value using the previous signal values, over a predictive distance. An optimized operator is used to remove the predicted regular signal so that the events such as defects can be extracted and investigated more easily.

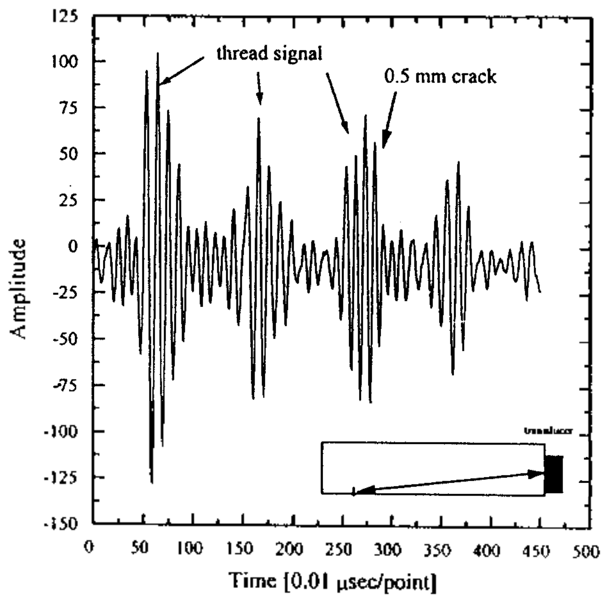

Figure 6. Ultrasonic signal from threads with a crack.

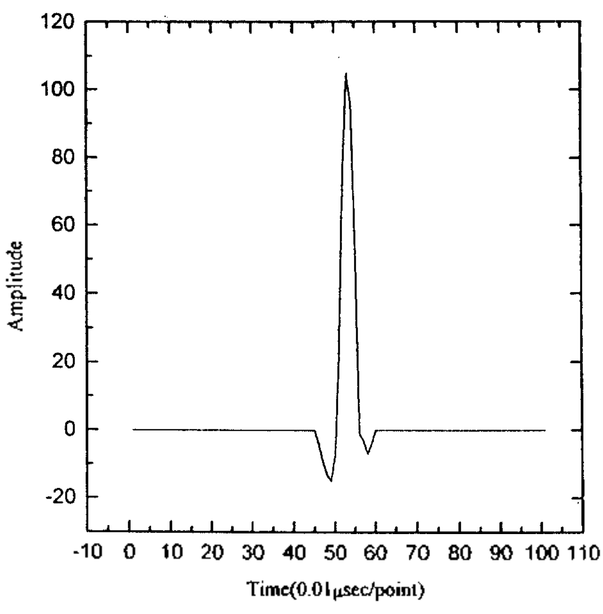

Figure 7. Desired signal.

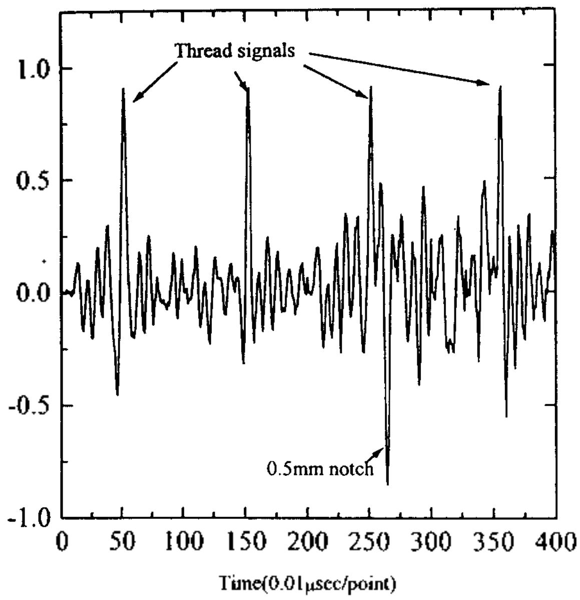

Figure 8. Processed signal by the proposed wave shaping method.

After briefly summarizing the predictive deconvolution technique, we propose the dynamic predictive deconvolution method where the predictive distance for each prediction is adjusted from the previous predictive distance depending on the test environments.

A. Predictive Deconvolution

If it takes T_1 seconds for an ultrasonic wave to travel from a thread root to the next thread root, the time interval between two consecutive echoes is $2T_1$. Let the incident wave from the transducer to the threads is $x(t)$. Then the reflected wave $R(t)$ from the threads can be expressed as

$$R(t)=\sum_{k=1}^{N} R_k x(t-2kT_1), \tag{20}$$

where N is the number of threads and R_k is the amplitude of the reflected wave determined by the attenuation characteristics of the threads.

Let $R(n)$ be the sampled version. If the length of the prediction operator p is $m+1$ and the number of sample points corresponding to the distance between two consecutive thread roots is D, then the error between the actual signal and the predicted signal (for example, the error between R_2 and estimated R_2 predicted from R_1 in Fig. 1) can be expressed as

$$E=\sum_{n=0}^{D-1}\left(R(n+D)-\sum_{s=0}^{m} p(s)\,R(n-s)\right)^2. \tag{21}$$

The optimized prediction operator can be found by

$$\frac{\partial E}{\partial p(n)}=0, \quad n=0,1,\cdots,m, \tag{22}$$

From (22),

$$\sum_{s=0}^{m}\sum_{n=0}^{D-1} p(s)R(n-j)R(n-s)=\sum_{n=0}^{D-1} R(n+D)R(n-j),$$

$$j=0,1,\cdots,m. \tag{23}$$

By defining r_{j-s} as

$$r_{j-s}=\sum_{n=0}^{D-1} R(n-j)R(n-s), \tag{24}$$

(23) can be expressed as

$$\sum_{s=0}^{m} p(s)r_{j-s}=r_{j+D}, \quad j=0,1,\cdots,m. \tag{25}$$

Thus the optimized coefficients of p(n) can be obtained by solving the following matrix equation:

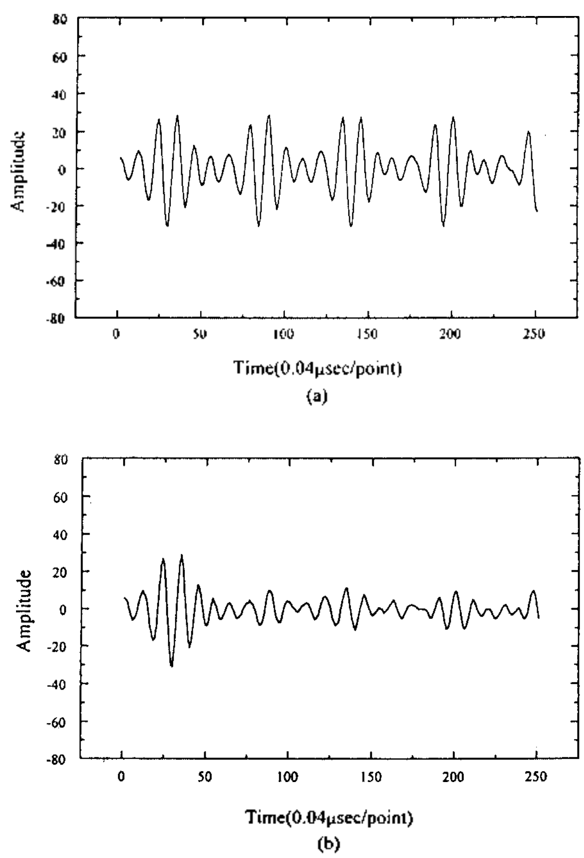

Figure 9. Application example of predictive deconvolution technique; (a) signal received at a transducer, (b) processed signal by predictive deconvolution.

$$\begin{bmatrix} r_0 & r_1 & \cdots & r_m \\ r_1 & r_0 & \cdots & r_{m-1} \\ \vdots & \vdots & \ddots & \vdots \\ r_m & r_{m-1} & \cdots & r_0 \end{bmatrix} \begin{bmatrix} p(0) \\ p(1) \\ \vdots \\ p(m) \end{bmatrix} = \begin{bmatrix} r_D \\ r_{D+1} \\ \vdots \\ r_{D+m} \end{bmatrix}. \tag{26}$$

Using the optimized coefficients, the estimated value for $R(n+D)$ can be computed as $\sum_{s=0}^{m} p(s)\,R(n-s)$.

An application example of the predictive deconvolution technique is shown in Fig. 9. Fig. 9(a) shows an ultrasonic signal obtained from threads without any crack. By applying the predictive deconvolution technique to the signal in Fig. 9(a), the processed signal in Fig. 9(b) is obtained. From Fig. 9(b), it is easy to see that there are no cracks in the threads under inspection.

B. Dynamic Predictive Deconvolution

In conventional predictive deconvolution technique, it is assumed that the prediction distance D is constant. Although this assumption is valid for many applications, D often needs to be adjusted to $D+\delta_i$ for the i-th prediction depending on the location of the transducer, the structure of bolt threads, and the sampling frequency.

Consider Fig. 10 which shows the location of the transducer and the structure of thread roots. The distance d_i from the transducer to the i-th thread root is

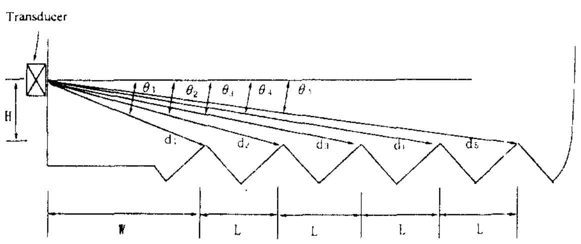

Figure 10. A test environment showing the location of the transducer and the various distances to the thread roots.

$$d_i = \frac{W+(i-1)L}{\cos\theta_i}. \tag{27}$$

The angle θ_i can be computed as

$$\theta_i = \tan^{-1}\left(\frac{H}{W+(i-1)L}\right). \tag{28}$$

In the proposed dynamic predictive deconvolution method, the prediction distance is adjusted for each prediction using (27) and (28).

In the predictive deconvolution method, prediction for the k-th signal $R_k x(t-2kT_1)$ is performed based on the $(k-1)$-th signal $R_{k-1}x(t-2(k-1)T_1)$. However, if the $(k-1)$th signal contains errors, the prediction for the k-th signal cannot be accurate. Thus, in the proposed dynamic predictive deconvolution method, each prediction is performed based on the first received signal $R_1 x(t-2T_1)$.

The signal in Fig. 11(a) was obtained by applying predictive deconvolution to a signal collected from a test specimen which has a crack only at the third thread root. Although the processed signal clearly shows that the third thread root has a crack, it does not give accurate information after the third thread root. The signal in Fig. 11 (b) was obtained by applying dynamic predictive deconvolution to the signal collected from the same specimen. Fig. 11(b) clearly shows that the test specimen has a crack only at the third thread root.

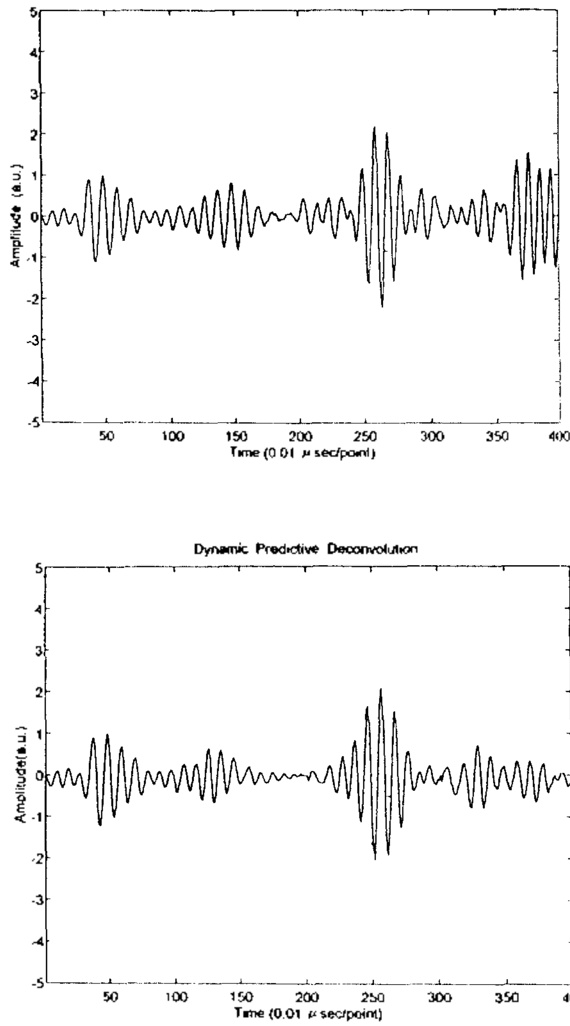

Figure 11. Comparison of the results of predictive deconvolution and dynamic predictive deconvolution; (a) signal processed by predictive deconvolution, (b) signal processed by dynamic predictive deconvolution.

V. Dynamic Predictive Deconvolution Combined with Wave Shaping

By wave shaping, it is possible to enhance the sharpness of ultrasonic waveforms. Dynamic predictive deconvolution can be applied to the wave-shaped signals to give clearer picture of the conditions of a stud (bolt). An application example of the dynamic predictive deconvolution combined with wave shaping is shown in Fig. 12. Fig. 12 (a) shows an ultrasonic signal obtained from threads without any crack. By applying the wave shaping technique to the signal in Fig. 12(a), the wave-shaped signal in Fig. 12 (b) is obtained. The signal in Fig. 12(c) is obtained by applying the dynamic predictive deconvolution technique to the wave-shaped signal in Fig. 12(b). From Fig. 12(c), it is easy to see that there are no cracks in the threads under inspection.

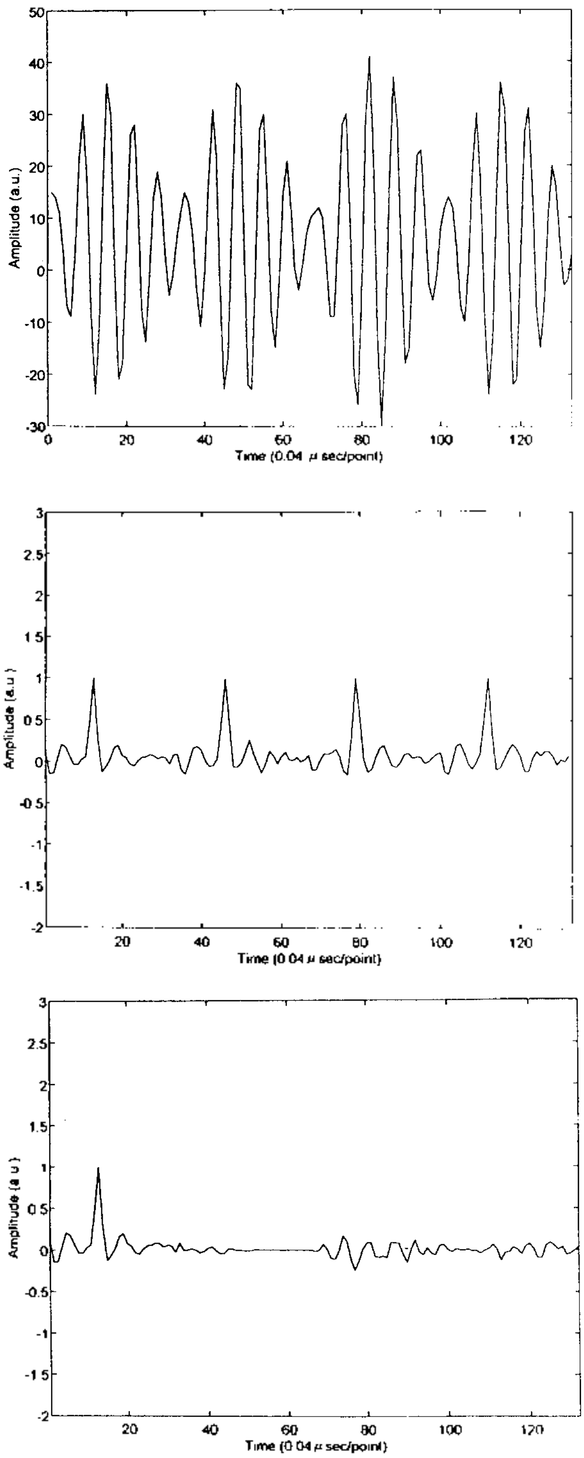

Figure 12. Dynamic predictive deconvolution combined with wave shaping; (a) signal received at a transducer, (b) processed signal by wave shaping, (c) further processed signal by dynamic predictive deconvolution.

VI. Conclusions

We have proposed a method by which we can detect and size very small cracks in the thread roots of studs and bolts. The key idea is from the observation that the Rayleigh wave propagates slowly along a crack from the tip to the opening and is reflected from the opening mouth. When there exists a crack, a small delayed pulse due to the Rayleigh wave is detected between large regularly spaced pulses from the thread. The delay time is the same as the propagation delay time of the slow Rayleigh wave and is proportional to the size of the crack. In spite of the complex geometry of the threads of a stud bolt, the Rayleigh wave technique can identify a small crack in the root of the threads (as small as 0.5mm).

To efficiently detect the slow Rayleigh wave, three methods based on the digital signal processing techniques have been proposed: modified wave shaping, dynamic predictive deconvolution, and dynamic predictive deconvolution combined with wave shaping. The effectiveness of these methods has been demonstrated by several examples.

In general, there are a large number of bolts in a system. Thus, for some applications, it is crucial to decrease the time needed for ultrasonic test. To this end, the fabrication of ASIC (Application-Specific Integrated Circuit) for dynamic predictive deconvolution combined with wave shaping is currently under study.

Also, it is expected that the proposed methods can be used for ultrasonic inspection of other materials. Obviously, some modifications will be necessary depending on the characteristics of the test material.

References

1. G. M. Light, "Ultrasonic detection of stress-corrosion cracks

in reactor pressure vessel and primary coolant system anchor studs(bolts)," *Mater. Eval.*, pp. 1413-1418, 1987.
2. NUREG-1339, "Resolution of generic safety issue 29 : bolting degradation or failure in nuclear power plants," *U.S. Nuclear Regulatory Commission*, June 1990.
3. NUREG-1445, "Regulatory analysis for the resolution of generic safety issue 29: bolting degradation or failure in nuclear power plants," *U.S. Nuclear Regulatory Commission*, Sept. 1991.
4. D. M. Suh and W. W. Kim, "A new ultrasonic technique for detection and sizing of small cracks in studs and bolts," *Journal of Nondestructive Evaluation*, vol. 14, no. 4, pp. 201-206, 1995.
5. D. Kishoni, "Application of digital pulse shaping by least squares method to ultrasonic signals in composites," *Review of Progress in Quantitative NDE*, pp. 781-787, 1986.
6. D. M. Suh, W. W. Kim, and J. G. Chung, "A Rayleigh wave technique for detection and sizing of small cracks in studs and bolts," in *Proceedings of 1996 IEEE Ultrasonics Symposium*, pp. 673-676, Nov. 1996.
7. D. Kishoni, "Removal of dominant reverberations from ultrasonic time-records of layered material by digital predictive deconvolution," in *Proceedings of 1987 IEEE Ultrasonics Symposium*, pp. 1075-1078, 1987.

▲Dong-Man Suh

Dong-Man Suh received the B.S. degree and the M.S. degree from the Chonbuk National University, in 1985 and 1992, respectively, and the Ph.D. degree in 1997 from the Chungnam National University, all in Electronics Engineering. From 1985 to 1995, he worked on Nondestructive Testing at the Korea Atomic Energy Research Institute. Currently, he is an assistant professor at Kunjang College. His research interests include crack sizing and signal processing in NDT.

▲Whan-Woo Kim

Whan-Woo Kim was born in Chonju, Korea, on September 20, 1954. He received the B.S. degree in electronics engineering from Seoul National University, in 1977, the M.S. degree in electrical and electronics engineering from Korea Advanced Institute of Science and Technology, in 1979, and the Ph.D. degree in electrical engineering from University of Utah, in 1988. While in graduate school at University of Utah, he worked on acoustic inverse scattering computerized tomography.

Since April 1979, he has been with the Department of Electronics Engineering at Chungnam National University, where he is a Professor. His research interests are on signal restoration and processing, signal processing in digital communication and mobile communication.

▲Dae-yen Kim

Dae-yen Kim received the B.S. degree and the M.S. degree from the Chonbuk National University, in 1996 and 1998, all in Communication Engineering. He is currently with Samsung Advanced Institute of Technology developing digital communication modems.

His current research interests include digital communication, digital signal processing and vlsi design.

▲Jin-Gyun Chung

Jin-Gyun Chung received the B.S. degree in electronics engineering from Chonbuk National University, Chonju, South Korea, in 1985, and the M.S. and Ph.D. degrees in electrical engineering from the University of Minnesota, Minneapolis, in 1991 and 1994.

He has been with Chonbuk National University, since 1995, where he is currently an Assistant Professor of Information & Communication Engineering.

His research interests are in the area of VLSI architectures and algorithms for signal processing, which includes the design of high-speed algorithms for digital filters, coding systems and speech and image processing systems.